

# Distribution and related dynamics of high-risk conjunction events in LEO

Rachit Bhatia, Darren McKnight, Erin Dale, and Mohin Patel  
*LeoLabs Inc.*

## ABSTRACT

Space Domain Awareness (SDA) is the technical capability to collect, analyze, and process the data pertaining to the objects in space such that a continuous catalog of their activities and operational environment can be maintained. Many studies, especially in recent years, have focused on the population distribution of the space objects and the associated conjunction risk, however, the studies to understand the distribution of the conjunction events (specifically high-risk events) have been relatively fewer in number.

This study presents the latitude/longitude distribution of the high-risk (probability of collision  $\geq 1e-6$ ) conjunction events in the Low Earth Orbit (LEO, region between 300 and 2,000 km altitude) over 1.5 years time-period and this distribution is analyzed with respect to various parameters, including conjunction type, event altitude, probability of collision, miss distance, inclination, and eccentricity of the two objects, respectively.

Latitudinal distribution, for all high-risk conjunction alerts, shows characteristic peaks near 50 degrees North and South, along with smaller spikes around polar regions. Whereas, for the longitudinal distribution, the high-risk events are almost uniformly distributed. While the average distribution for all high-risk conjunction alerts do not change with time, the distribution varies for other parameters, like latitudinal distribution for conjunctions between two fragments is different from that between two operational payloads. This kind of detailed analyses can help understand inherent trends and provide useful insights. This distribution is studied over 1.5 years time-period and the changes due to orbital decays and/or geolocation of the sensor network are noted.

Distribution of the classical orbital elements (specifically the inclination and eccentricity at the time of closest approach) of the objects involved in high-risk conjunction events is presented for two specific sub-groups, i.e., Cosmos 1408 fragment cloud and SL-16 rocket body cluster. The trends are analyzed and discussed with respect to various parameters. Lastly, the comparison of the distribution for the events tracked by LeoLabs and Combined Space Operations Center (CSPOC) is presented and corresponding insights about conjunction event detectability is shared.

The global network of two UHF and eight S-band radars, built and operated by LeoLabs, provide a 24/7 data feed to power this assessment and help identify the evolution of these events and related dynamics. The ability to access this data in near real-time, and provide necessary alerts and services to the customers, significantly enhance operational safety, and enable investigation of specific impacts on different subgroups.

Key aspects of this study are aimed at improving understanding of the distribution of high-risk events in LEO and identifying underlying dynamics/parameters. The goal is to provide necessary intuition to the reader about the evolution of this risk and check the feasibility of using this newly gained intuition to gain insights about future events.

## 1. MOTIVATION

An important component of SDA involves leveraging dynamic knowledge of the environment to estimate and mitigate future risks. Dynamic knowledge for LEO becomes critical because of unique challenges and characteristics associated with this orbital region. Thus, a global sensor network coupled with vertically integrated space operations stack becomes necessary to provide continuous, scalable, reliable, transparent, traceable, and insightful solutions to enable space safety.

LeoLabs is a commercial provider of LEO mapping and Space Situational Awareness (SSA) services with its own global radar network and data platform. LeoLabs' tracking and monitoring delivers high accuracy tracking data

products for satellites down to 1U or slightly smaller. [1] Currently, the radar network is comprised of phased-array radars, appropriately located around the globe. The near real-time tracking data and conjunction alerts being generated by such a wide network provides a basis for the development of innovative statistical methodologies aimed at identification of patterns and extraction of insights pertaining to the interplay of conjunction events, their grouping, clustering, and how these patterns evolve over time.

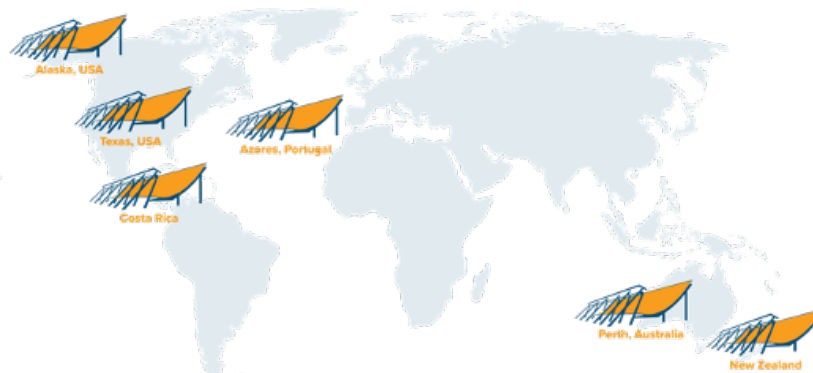


Figure 1: LeoLabs global radar coverage.

A number of studies have evaluated and characterized clustering of orbital debris in GEO, specifically looking into inherent dynamics leading to increased debris fluxes through particular longitude slots. [2, 3, 4, 5] However, such evaluations for LEO regime have been uncommon mostly because it is more dynamic and chaotic. LEO orbits are characterized by large perturbations due to gravity and atmospheric drag, higher orbital velocities, and shorter orbital periods, respectively. Thus, making the trajectories of LEO resident space objects (RSOs) more dispersed. With that being stated, many patterns emerge because of specific regions (like particular altitudes or inclinations) in LEO which are distinctively dominated by specific object types, for example, region between 850-950 km being dominated by large rocket bodies. Analyzing conjunction patterns in these regions can provide useful insights for modeling small debris, quantifying and predicting conjunction risk, estimating long term sustainability, and planning mitigation strategies. [6, 7]

Only a few studies were found to explore latitudinal/longitudinal distribution of conjunction risk due to small debris in LEO. [8] Thus, this investigation is focused on utilizing rich corpus of conjunction alert data produced over 1.5 years time-period to assess current trends relative to specific parameters of interest, including latitude/longitude/altitude of given conjunction event and inclination/eccentricity of the objects involved.

In the following section, results are shown for latitudinal, longitudinal, and temporal distribution of different types of conjunction events, involving specific object types or sub-groups of LEO RSOs. Discussion on trends observed and possible causes are included. In section 3, dynamic characterization of two specific sub-groups, Cosmos 1408 fragment cloud and SL-16 rocket body cluster, is done by analyzing frequency distribution and trends for CDM source, miss distance, collision probability, and specific orbital parameters with respect to latitude, longitude, and temporal parameters. The trends for these two distinct sub-groups are compared to gain insights about LEO dynamics. Lastly, a summary is presented to discuss and emphasize key aspects of this study.

For some results shown in section 2 and 3, the coordinate system has been defined such that the equator is at 90 degrees latitude and the poles are at 0 and 180 degrees latitude, respectively. Further, the Prime Meridian, i.e., 0 degrees longitude, is located in Greenwich, England, and longitude increases eastward up to 360 degrees, respectively. This representation has been adopted to help focus on specific hemispheres and to simplify calculations. It's important to note that the fundamental principles of latitude and longitude remain the same, but the values are interpreted differently in this coordinate system. The caption for the figures, with changed coordinate system, highlight the use of different convention.

## 2. LATITUDINAL AND LONGITUDINAL DISTRIBUTION

In this section, temporal distribution, with respect to latitude/longitude, for high-risk conjunction alerts involving different subgroups is presented. The severity of risk for a particular conjunction alert has been defined based on probability of collision ( $P_c$ ) for the latest conjunction data message (CDM) published for the given event. For this study, any conjunction event with  $P_c$  greater than or equal to  $1e-6$  is specified as a “high-risk” event. For this study, high-risk conjunction alerts with the time of closest approach (TCA) between 1st Jan 2022 and 30th June 2023 are considered.

In Figures 2 and 3, temporal distribution of all high-risk conjunction events with respect to latitude and longitude of the event at the time of closest approach is presented. While the longitudinal distribution is fairly uniform, the latitudinal distribution is interesting because of characteristic peaks near 50 degrees North and South, along with smaller spikes around polar regions. This distribution pattern means the likelihood of a high risk conjunction event is higher at these latitudes. High spatial density in these regions can either be due to large population of RSOs in these regions or lower volumetric density or both.

The spike at the polar region is mostly due to lower volumetric density caused because of orbital geometry and inclination angles. The trajectories of satellites orbiting close to poles converge towards the pole and their paths become constricted, thereby reducing the coverage area at higher latitudes and increasing the likelihood of a high risk conjunction. This is in contrast to a LEO satellite with inclinations closer to equator because their trajectories are oriented at an angle to the Earth’s rotational axis, allowing them to cover a wider area.

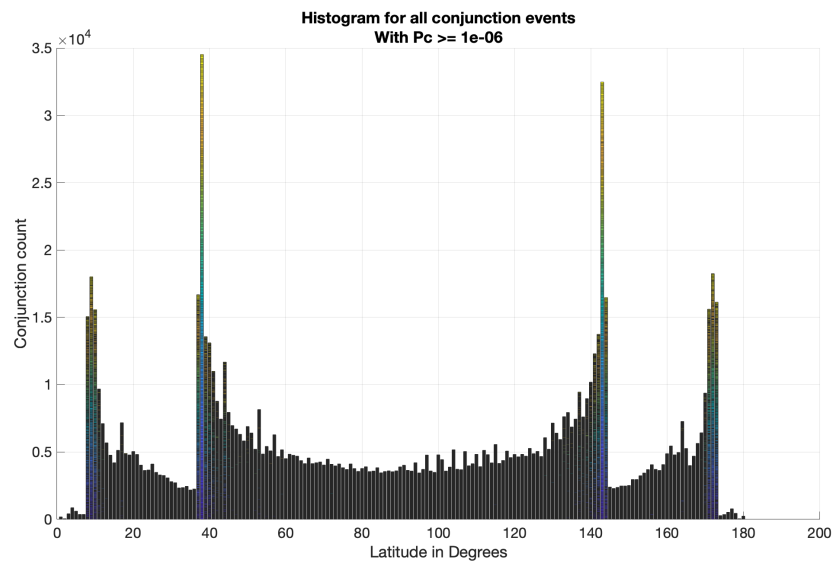


Figure 2: Temporal distribution of all high-risk ( $P_c \geq 1e-6$ ) conjunction events with respect to event latitude. Color variation (from blue to yellow) highlights the increase in conjunction count. Note that the coordinate system has been defined such that the equator is at 90 degrees latitude and the poles are at 0 and 180 degrees latitude, respectively.

Regarding the spike at 50 degree North and South latitude in Fig. 2, it is suspected to be because of the increased population of RSOs in this region. This reasoning is verified when latitudinal distribution of all high-risk conjunction events involving two operational satellites is compared with the same for two derelict objects.

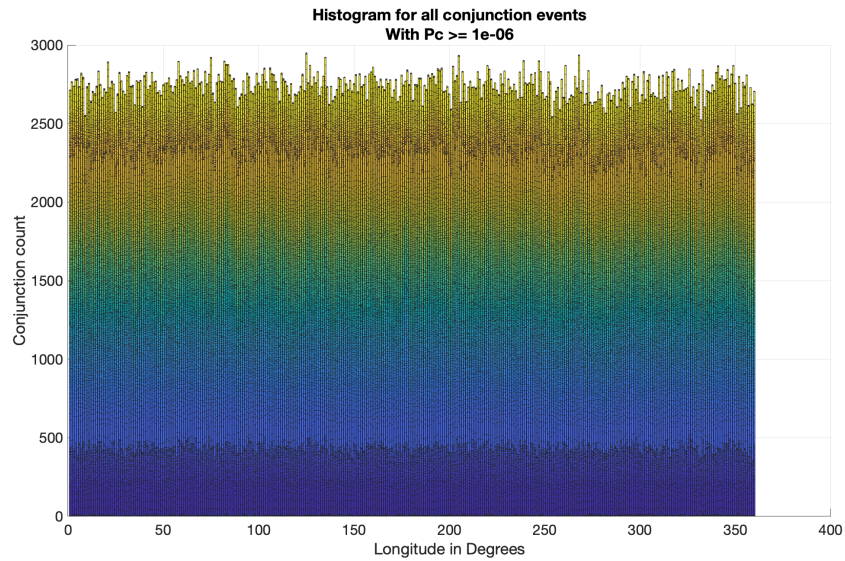


Figure 3: Temporal distribution of all high-risk ( $P_c \geq 1e-6$ ) conjunction events with respect to event longitude. Color variation (from blue to yellow) highlights the increase in conjunction count. Note that the coordinate system has been defined such that the Prime Meridian, i.e., 0 degrees longitude, is located in Greenwich, England, and longitude increases eastward up to 360 degrees, respectively.

In Figures 4 and 5, note how the spike at 50 degree North and South latitude disappears almost completely, for the conjunction alerts involving two derelicts, thus verifying the reason for this trend to be due to increased RSO population. Interestingly, the spike at poles for the conjunction alerts involving two operational satellites does not disappear and this proves that the heightened risk at poles is inherently connected to orbital geometry.

It is also important to point out that while the increased RSO population is responsible for the increased conjunction count at 50 degree North and South latitude, this is generally mitigable risk as most of these RSOs are operational and are designed to consistently perform risk reduction maneuvers to maintain safe orbital configuration. Thus, conjunction risk at poles is more challenging than that at 50 degree North and South latitude.



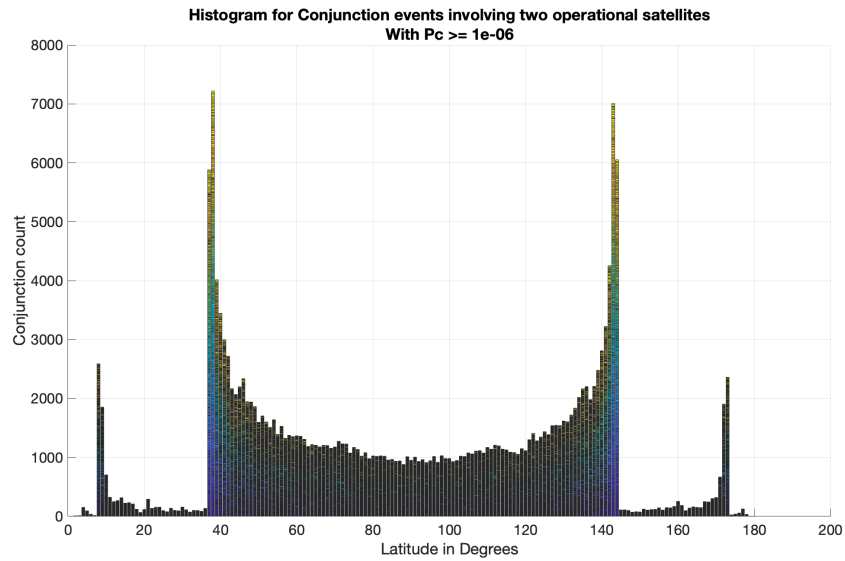


Figure 4: Temporal distribution of all high-risk ( $P_c \geq 1e-6$ ) conjunction events involving two operational satellites with respect to event latitude. Color variation (from blue to yellow) highlights the increase in conjunction count. Note that the coordinate system has been defined such that the equator is at 90 degrees latitude and the poles are at 0 and 180 degrees latitude, respectively.

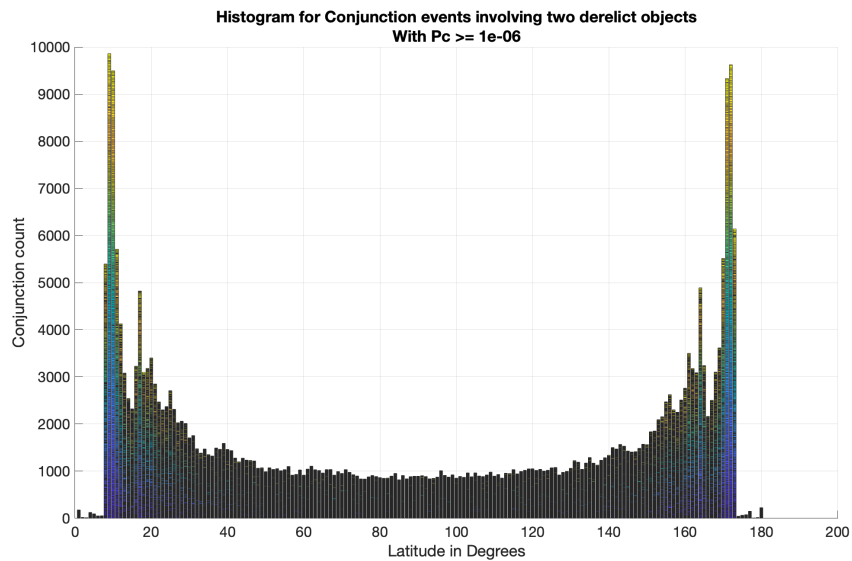


Figure 5: Temporal distribution of all high-risk ( $P_c \geq 1e-6$ ) conjunction events involving two derelict objects with respect to event latitude. Color variation (from blue to yellow) highlights the increase in conjunction count. Note that the coordinate system has been defined such that the equator is at 90 degrees latitude and the poles are at 0 and 180 degrees latitude, respectively.

Similarly, interesting trends emerge when similar distributions are studied for conjunction alerts involving other sub-groups, like Chinese rocket bodies (CZ series), Gaofen satellites, Iridium 33 fragments, and Cosmos 2251 fragments. Analysis of these results can facilitate understanding of constellation deployments or overall spread in case of a fragment cloud. Refer Figures 6, 7, 8, and 9.

For CZ rocket bodies, the event count is spiking at 30, 50, and 90 degrees North and South, respectively. The two peaks at 30 and 50 degrees highlight the orbital distribution of these rocket bodies. Whereas, for Gaofen satellites, the trends are very similar to that for the scenario involving two operational satellites. The difference in event count at poles versus that at 50 degrees North and South in Fig. 7, can help provide insights about the type of objects involved in conjunctions with Gaofen satellites and overall variation in conjunction risk.

The variation in altitude versus latitude/longitude distribution of conjunction events involving Iridium 33 and Cosmos 2251 fragment clouds is shown in Figures 8 and 9. Since both of these fragment clouds were generated during the same event, it is useful to compare the distribution and infer some characteristics about the orbital spread, fragment population, and spatial density. Clearly, the fragment cloud for Iridium 33 is more widely spread than that for Cosmos 2251. This means that the spatial density of Iridium 33 is lower than that of Cosmos 2251 cloud, which is in line with observations as only ~240 Iridium 33 fragments remain in orbit compared to ~962 in-orbit fragments for Cosmos 2251, as of August 2023.

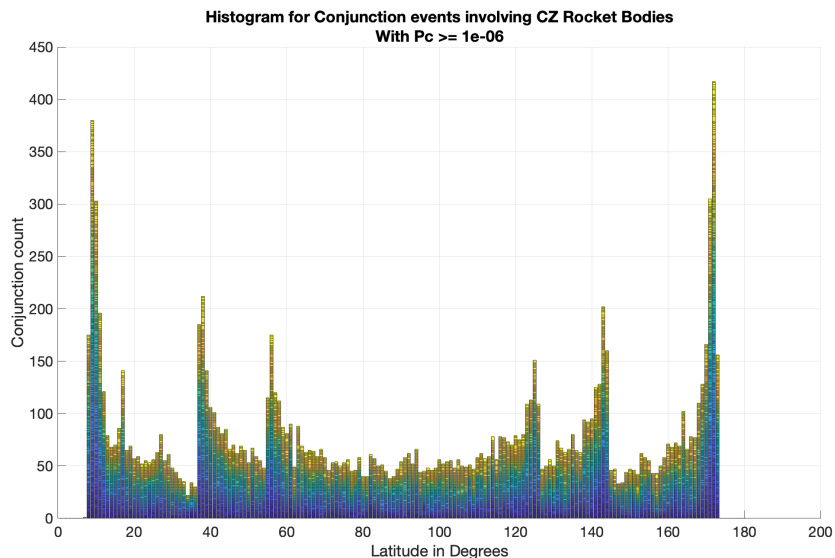


Figure 6: Temporal distribution of all high-risk ( $P_c \geq 1e-6$ ) conjunction events involving CZ-series rocket bodies with respect to event latitude. Color variation (from blue to yellow) highlights the increase in conjunction count. Note that the coordinate system has been defined such that the equator is at 90 degrees latitude and the poles are at 0 and 180 degrees latitude, respectively.

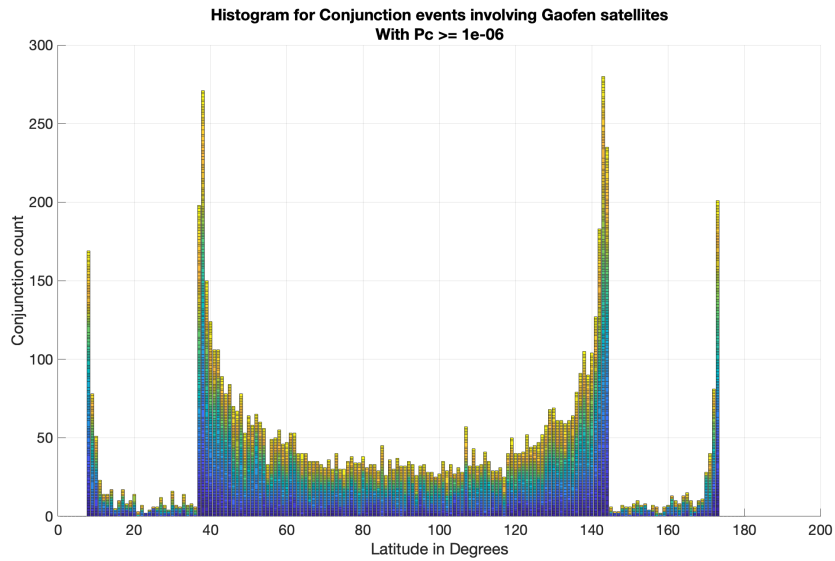


Figure 7: Temporal distribution of all high-risk ( $P_c \geq 1e-6$ ) conjunction events involving Gaofen satellites with respect to event latitude. Color variation (from blue to yellow) highlights the increase in conjunction count. Note that the coordinate system has been defined such that the equator is at 90 degrees latitude and the poles are at 0 and 180 degrees latitude, respectively.

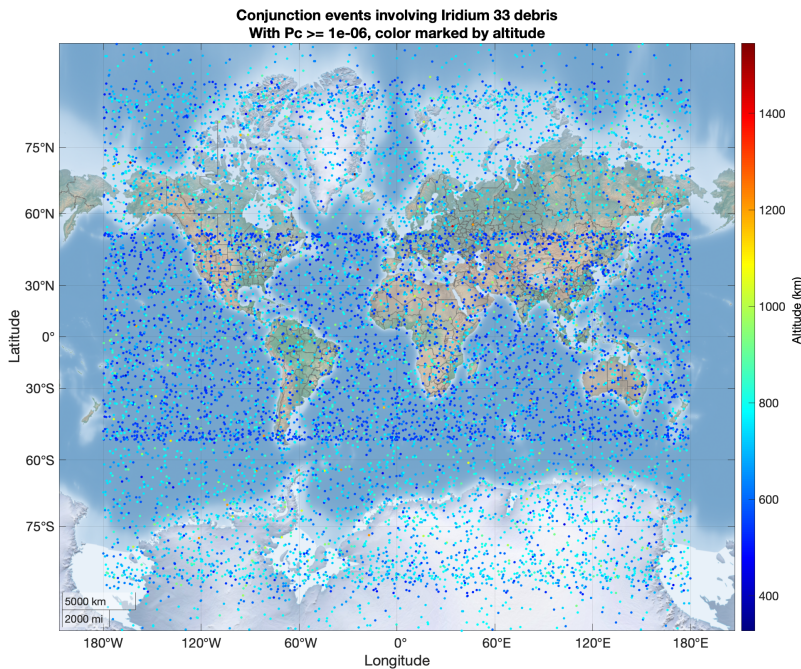


Figure 8: Altitudinal distribution of all high-risk ( $P_c \geq 1e-6$ ) conjunction events involving Iridium 33 fragments with respect to event latitude and longitude. Color variation highlights altitude in km.

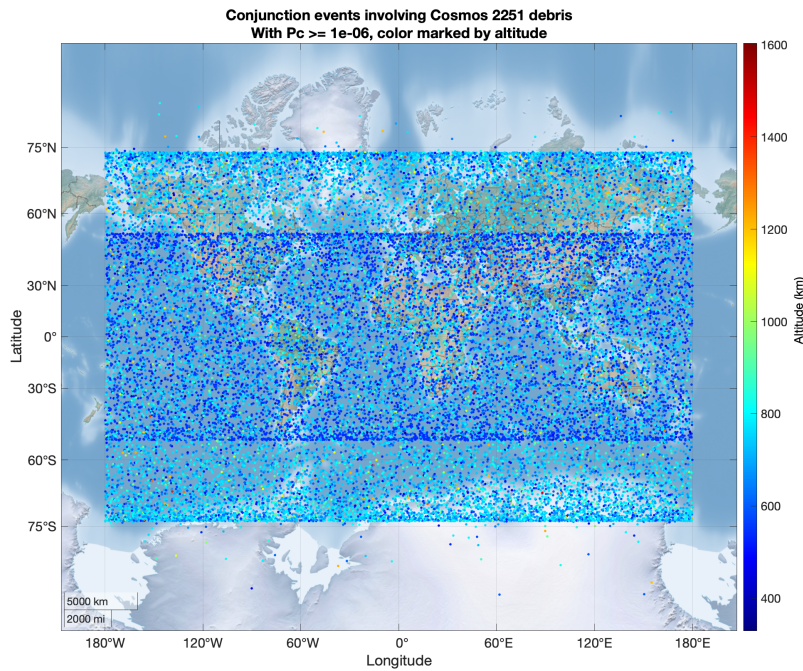


Figure 9: Altitudinal distribution of all high-risk ( $P_c \geq 1e-6$ ) conjunction events involving Cosmos 2251 fragments with respect to event latitude. Color variation highlights altitude in km.

### 3. DYNAMIC CHARACTERIZATION

In this section, dynamic characterization of a fragment cloud and rocket body cluster is presented, and parametric comparison is conducted to highlight clustering and dispersion of the high risk conjunction events. The results shown here help infer underlying dynamics governing the spread of a fragment cloud and evolution of a rocket body cluster. This is helpful to understand risk modeling for “bad neighborhoods” and improve methods for statistical risk assessment. [6]

To understand the spread of the cloud, variation in altitude with respect longitude over 1.5-year time period is shown for high-risk conjunctions involving Cosmos 1408 fragments, see Fig. 10. A distinct band around ~580 km suggests that the encounter rate due to Cosmos 1408 cloud peaked at this altitude. This is in line with various analyses conducted for this event. [9]

Similar, observations are made for SL-16 rocket body cluster where the band is at ~820 km altitude, see Fig. 11. However, the altitudinal spread for SL-16 rocket bodies is much smaller than that for Cosmos 1408 fragment cloud. Also, two faint bands, around ~1000 km and ~620 km, are visible for SL-16 R/B cluster, indicating a stable population of SL-16 rocket bodies at these altitudes.

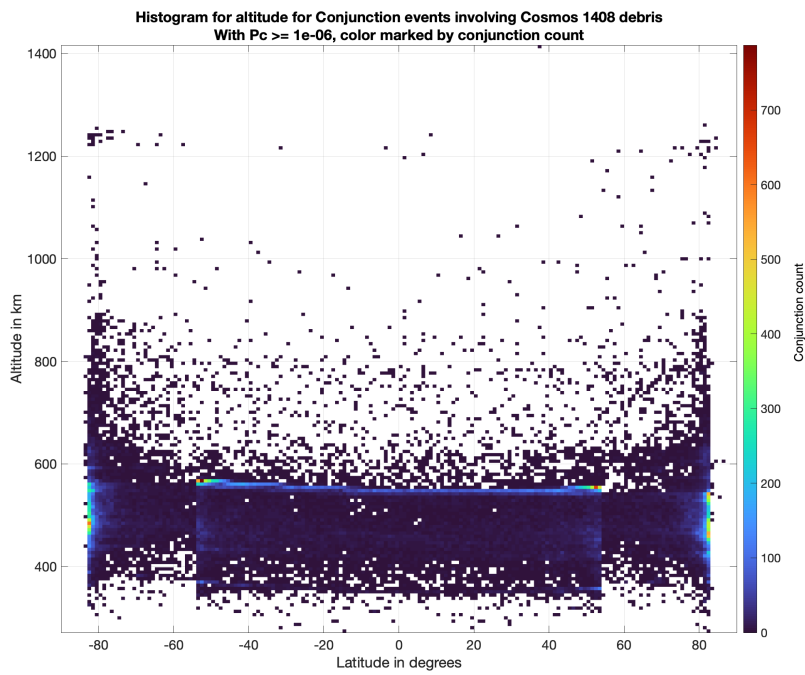


Figure 10: Altitudinal distribution versus event latitude of all high-risk ( $P_c \geq 1e-6$ ) conjunction events involving Cosmos 1408 fragments.

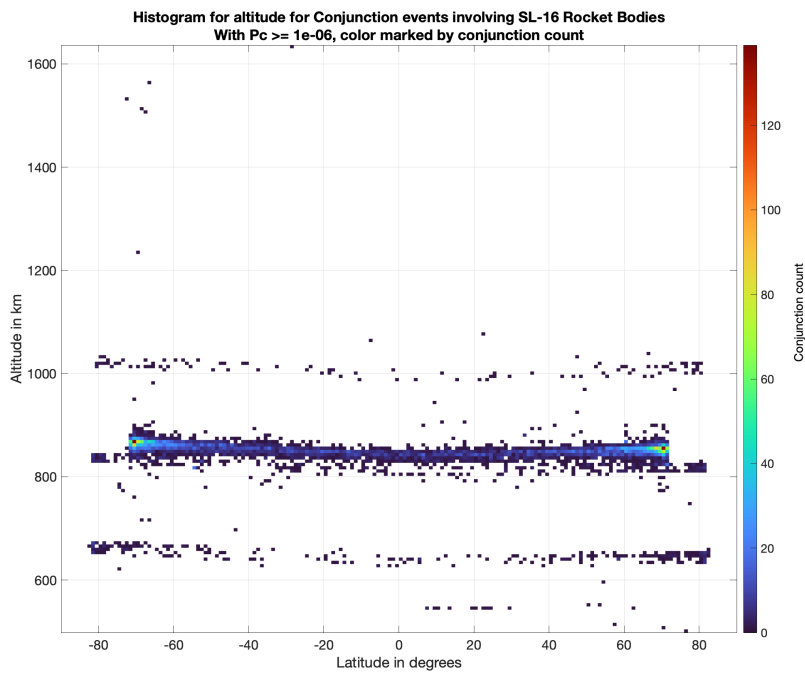


Figure 11: Altitude distribution versus event latitude of all high-risk ( $P_c \geq 1e-6$ ) conjunction events involving SL-16 rocket bodies.

Next, the severity of the conjunctions being encountered due to fragment cloud and rocket body cluster can be quantified by studying the distribution of miss distance versus event latitude, see Figures 12 and 13.

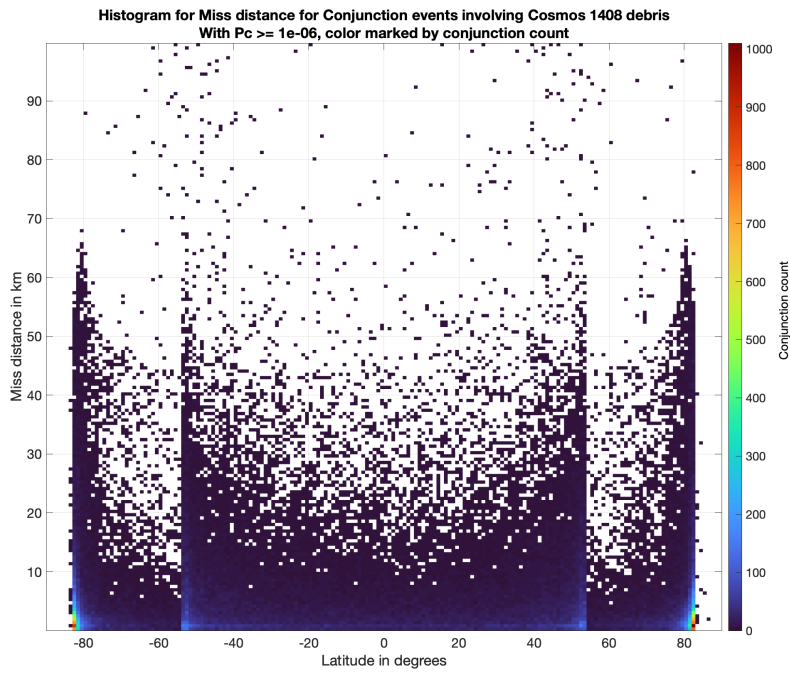


Figure 12: Miss distance distribution versus event latitude of all high-risk ( $P_c \geq 1e-6$ ) conjunction events involving Cosmos 1408 fragments.

In both cases, the spike in conjunction risk and frequency near polar latitude, as observed in latitudinal distribution, can be noted. The increased conjunction activity for Cosmos 1408 fragment cloud near 50 degrees North and South latitude quantifies the risk posed by this event to the operational satellites.

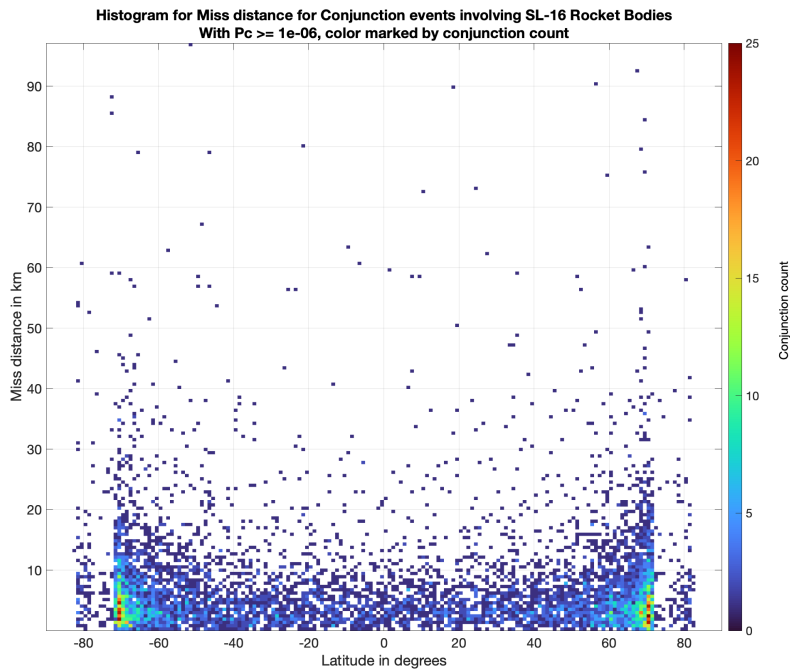


Figure 13: Miss distance distribution versus event latitude of all high-risk ( $P_c \geq 1e-6$ ) conjunction events involving SL-16 rocket bodies.

Further, the distribution of secondary object's eccentricity and inclination is studied with respect to the event latitude for both fragment cloud and rocket body cluster. Distinct bands are noted in both distributions, see Figures 14 and 15.

For Cosmos 1408 fragment cloud, the bands form a dome-like shape, such that conjunction count is higher for lower eccentricities at higher latitudes and decreases for higher eccentricities at higher latitudes. Whereas for SL-16 rocket body cluster, the bands are linear and concentrated to a smaller range relative to the spread for Cosmos 1408 fragment cloud.

The peculiar shapes of these distributions highlight the differences between a decaying fragment cloud and stable rocket body cluster, as orbits of fragments are circularized due to the effects of atmospheric drag, whereas SL-16 rocket bodies continue to maintain stable orbits because of their higher altitudes.

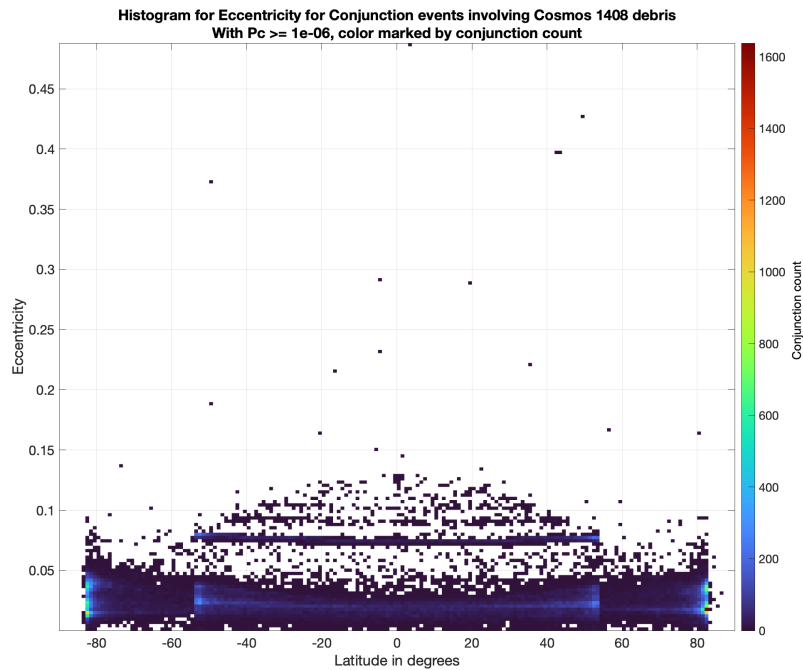


Figure 14: Eccentricity distribution versus event latitude of all high-risk ( $P_c \geq 1e-6$ ) conjunction events involving Cosmos 1408 fragments.



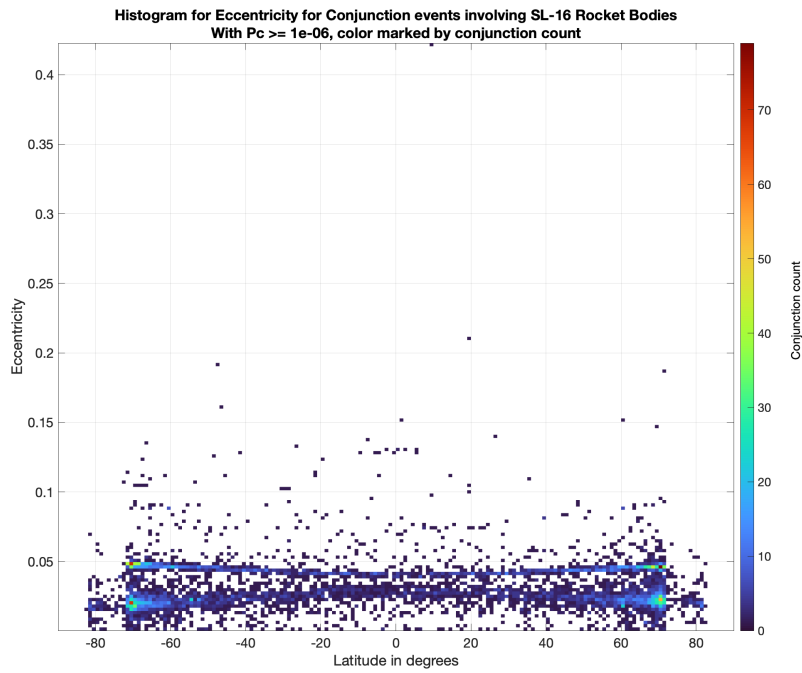


Figure 15: Eccentricity distribution versus event latitude of all high-risk ( $P_c \geq 1e-6$ ) conjunction events involving SL-16 rocket bodies.

In contrast to varying patterns noted in eccentricity distributions, trends in inclination distribution for the fragment cloud and rocket body cluster are similar and only highlight the orbital spread of each group. Refer Figures 16 and 17.

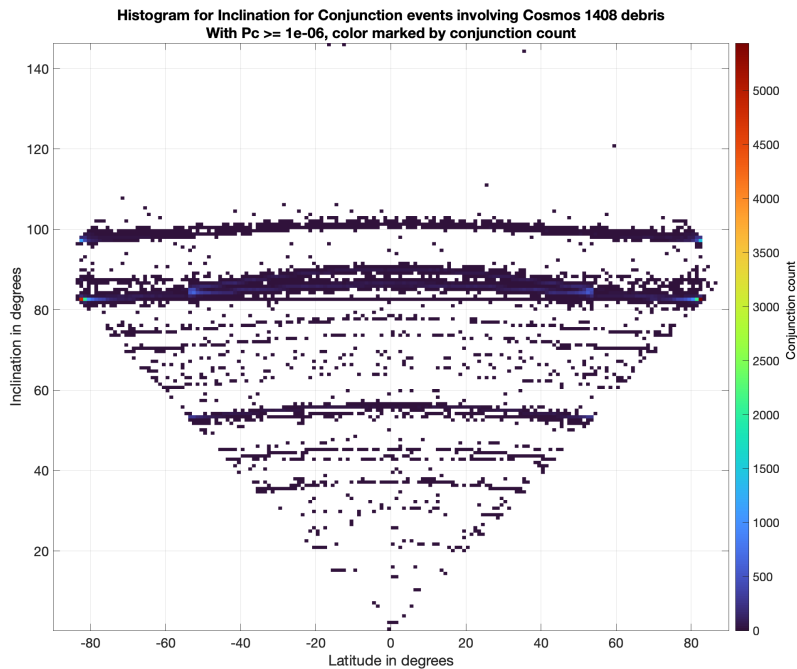


Figure 16: Inclination distribution versus event latitude of all high-risk ( $P_c \geq 1e-6$ ) conjunction events involving Cosmos 1408 fragments.

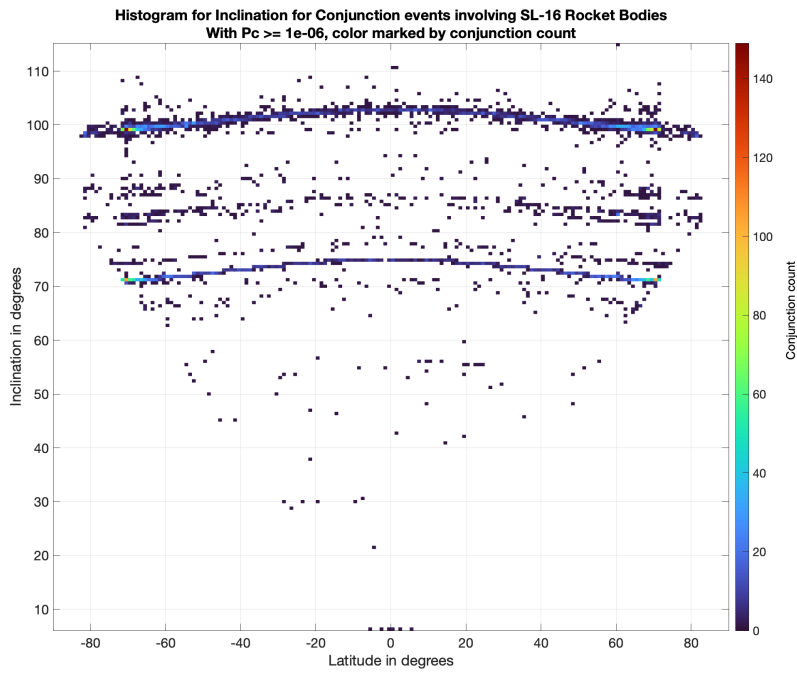


Figure 17: Inclination distribution versus event latitude of all high-risk ( $P_c \geq 1e-6$ ) conjunction events involving SL-16 rocket bodies.

Lastly, comparison of event detectability by two different SSA providers is shown in Fig. 18.

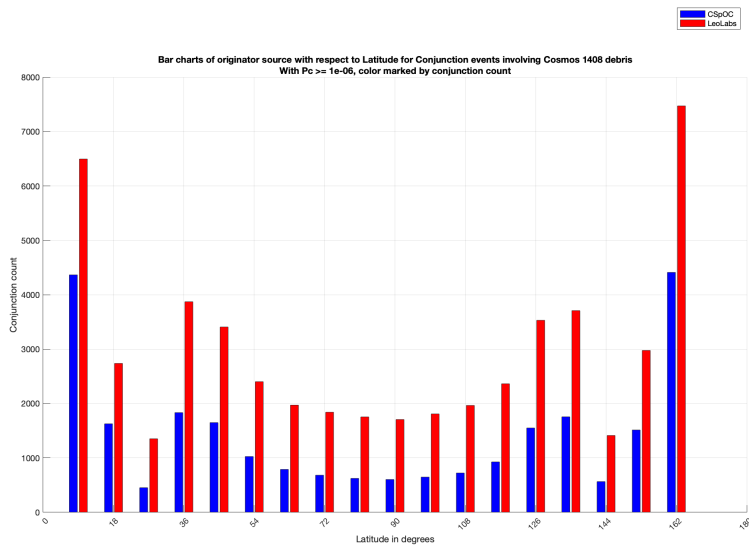


Figure 18: CDM source distribution versus event latitude of all high-risk ( $P_c \geq 1e-6$ ) conjunction events involving Cosmos 1408 fragments. Note that the coordinate system has been defined such that the equator is at 90 degrees latitude and the poles are at 0 and 180 degrees latitude, respectively.

The conjunction event frequency for each SSA provider is displayed with respect to event latitude and it can be noted how event detectability of LeoLabs network is almost 1.5x that of CSpOC network at each latitude for the conjunction events involving Cosmos 1408 fragments.

#### 4. CONCLUSION

A critical component of Space Domain Awareness (SDA) is comprehensive understanding of the dynamic environment. Dynamic knowledge of the environment requires continuous tracking of objects, characterization of behavior, and prediction of trajectories. Persistent surveillance of LEO by global radar network is essential in this regard. Consistent generation of reliable tracking data and conjunction alerts not only provide operational safety, but also form foundation for analyzing long term patterns, and identification of underlying parameters.

In this study, temporal/latitudinal/longitudinal distributions of high-risk conjunction alerts were analyzed, for different sub-groups of LEO RSOs, to highlight risk variation in LEO regime. Understanding of these patterns is expected to help satellite operators, mission planners, and regulators for optimizing orbital configurations for their missions, formulating risk reduction strategies, and long-term sustainability of LEO environment.

Parametric comparison for a fragment cloud and a rocket body cluster was also presented to highlight differences in evolution of different LEO neighborhoods and families. The results presented in this article provided reasonable insights about the variation in conjunction risk due to parameters like event latitude/longitude/eccentricity/inclination for different LEO RSOs. The effects of inherent dynamics of the environment and the overall impact on conjunction evolution patterns, clustering, and dispersion were presented and discussed.

#### REFERENCES

- [1] Rachit Bhatia, Darren Mcknight, Erin Dale, and Mr Patel. Assessment of evolving conjunction risk for small satellite missions. (08) 2023.
- [2] Paul V Anderson. *Characterizing Longitude-Dependent Orbital Debris Congestion in the Geosynchronous Orbit Regime*. PhD thesis, University of Colorado at Boulder, 2015.
- [3] Paul V Anderson, Darren S McKnight, FD Pentino, and Hanspeter Schaub. Operational considerations of geo debris synchronization dynamics. In *66th International Astronautical Congress, IAC-15 A*, volume 6, page 7. All Rights Reserved, 2015.
- [4] Darren S McKnight and Frank R Di Pentino. New insights on the orbital debris collision hazard at geo. *Acta Astronautica*, 85:73–82, 2013.
- [5] T Schildknecht, M Ploner, and U Hugentobler. The search for debris in geo. *Advances in Space Research*, 28(9):1291–1299, 2001.
- [6] Darren Mcknight, Rachit Bhatia, Ms Dale, Mr Kunstadter, Matthew Stevenson, and Mr Patel. A map of the statistical collision risk in leo. (09) 2022.
- [7] Matthew Stevenson, Darren McKnight, Hugh Lewis, Chris Kunstadter, and Rachit Bhatia. Identifying the statistically-most-concerning conjunctions in leo. In *2021 Advanced Maui Optical and Space Surveillance Technologies Conference (AMOS), Maui, Hawaii*, 2021.
- [8] Lieutenant Colonel Daniel Moomey, Rachael Falcon, and Arbab Khan. Trending and analysis of payload vs. all low earth conjunction data messages below 1000 km, from 2016 through 2021. *Journal of Space Safety Engineering*, 10(2):217–230, 2023.
- [9] Carmen Pardini and Luciano Anselmo. The short-term effects of the cosmos 1408 fragmentation on neighboring inhabited space stations and large constellations. *Acta Astronautica*, 2023.

#### TRANSFER OF COPYRIGHT

A signed statement of Transfer of Copyright has been attached with this paper.